International Journal of Original Recent Advanced Research
ISSN (Online): 3048-5479
Vol. 03, Issue 03, May 2026

STRUCTURAL DESIGN AND PERFORMANCE ANALYSIS OF A DELTA UAV CONFIGURATION

Sakharam Chouhan [1], Dr. Vishwjeet Ambade[2], Dr. Arepally Shushrutha[3]

Research Scholar, Department of Aeronautical Engineering, RTM Nagpur University[1]

Professor, Department of Aeronautical Engineering, RTM Nagpur University[2]

Professor, Department of Aeronautical Engineering, RTM Nagpur University[3]

ABSTRACT

This paper presents an empirical study to explore the aerodynamic, structural, and operational performance characteristics of erected Delta shaped Unmanned Aerial Vehicle (UAV) configurations, which constitute a hybrid structure based on the delta wing morphology, upon a bamboo-spine derived lattice reinforcement topology. The Delta UAV is a novel structural concept in which bioinspired skeletal frameworks are integrates classic swept-wing aerodynamics to attain improved lift-to-drag ratios, enhanced structural rigidity, and reduced overall structural weight. A systematic comparison of five primary structural configurations was conducted across key performance metrics, including drag coefficient (Cd), lift coefficient (Cl), structural stress distribution (von Mises stress), thrust-to-weight ratio (TWR), and endurance performance index (EPI), using a combination of computational fluid dynamics (CFD) simulation, finite element analysis (FEA), and wind tunnel experimental validation. A wind tunnel was used to collect experimental data over a range of Reynolds numbers (Re=3×105 to 1.2×106) and angle-of-attack (−4° to 20°) conditions. The results indicate an optimized Delta Type-3 airframe with a peak lift-to-drag ratio of 14.72, a von Mises peak stress of 38.4 MPa sustained under 3gs loading (well below safety margin) and 17.3% more endurance over comparable mass conventional delta-wing UAVs. The results show that there are statistically significant benefits of flight efficiency, structural stability and payload accommodation for bio-inspired lattice-reinforced delta configurations. However, in this research, a validated design framework has been presented for next-generation fixed-wing UAVs operating in surveillance, agriculture, and disaster management applications.

Keywords: *Delta UAV[1], swept-wing aerodynamics[2], bio-inspired lattice structure[3], CFD analysis[4], FEA structural simulation[5], lift-to-drag ratio[6], UAV endurance optimization[7].*

1. INTRODUCTION

1.1 Background and Motivation

Unmanned Aerial Vehicles (UAVs) have moved from a niche military application to be a vitally useful civilian resource, ranging from precision agriculture to infrastructure monitoring, disaster response, environmental surveying, and urban logistics. This acceleration has increased the demand for aerodynamically efficient, structurally sound and mass-optimized airframe designs. Conventional fixed-wing UAV designs typically win with rectangular or conventional delta planform which, whilst highly characterization in terms of aerodynamics, do create fundamental compromise with respect to structure and performance in a low-to-medium Reynolds number flight regimes. The structural configuration of Delta evolves from the dual offspring of two design philosophies: the classical delta wing-flapped design for inherent generation of high lift and hydrofoil tilt angle symmetry (which in portability sensors has ascertained phenomenal swept-wing stability characteristics), and the bamboo-spine lattice topology, a bio-inspired paradigm for structural reinforcement branched from the bamboo culm axial skeletal architecture. Bamboo has been acknowledged for its exceptional specific strength, specific flexural rigidity, and efficient load-spreading characteristics within structural engineering for many years. This morphological logic, when translated to UAV airframe design, theoretically allows for much higher stiffness-to-weight ratios without the more expensive composite layup manufacturing processes. Thus this study is motivated to quantify the performance gains, in both aerodynamic and structural aspects, of the Delta UAV configuration over conventional yielding means using both simulation and experimental techniques.

1.2 SCOPE AND OBJECTIVES

The scope of this research is confined to fixed-wing UAVs with a maximum takeoff weight (MTOW) of 5 kg, operating at altitudes between 50 m and 500 m AGL (above ground level) and cruise speeds ranging from 15 m/s to 35 m/s. The structural investigation focuses on composite frames integrating carbon fiber reinforced polymer (CFRP) outer skin panels with internal -patterned lattice ribs fabricated from polylactic acid (PLA) via fused deposition modelling (FDM). The aerodynamic analysis encompasses low-to-moderate Reynolds number regimes relevant to small UAV operations. The objectives of this study are: to design five geometrically distinct Delta UAV structural configurations with systematically varied sweep angle (45°–65°) and lattice rib density; to evaluate their aerodynamic coefficients, structural stress distributions, and endurance parameters through CFD, FEA, and wind tunnel testing; to statistically compare performance across configurations and against benchmark conventional delta UAVs; and to identify the optimal design configuration for surveillance and agricultural UAV applications. The study further aims to establish a replicable empirical methodology for bio-inspired UAV structural analysis that can guide future design iterations and manufacturing decisions.

1.3 SIGNIFICANCE OF THE STUDY

The Delta UAV is structurally novel and yet computationally underexplored design paradigm. While there is extensive literature on UAV aerodynamics, conventional delta, blended-wing-body and tandem-wing configurations have been investigated significantly compared to bio-inspired lattice-reinforced hybrid structures in the low-Reynolds-number fixed-wing UAV context. The fifth instantiates the current study, which addresses

this gap, via an experimental confirmed numerical data set that documents the performance envelope of Delta configurations vis-a-vis key aerodynamic and structural metrics/ Additionally, the practical implications of this work only serve to increase its significance: high-quality, low-cost airframe configurations that can be manufactured cheaply using FDM are of immediate concern to research facilities, compact UAV providers, and military research facilities seeking performance-optimized platforms with limited budgets [18,25]. In addition, a validated FEA-CFD co-simulation framework for bio-inspired UAV structures presents a generally applicatory contribution to the aerospace engineering community beyond the particular studies presented here.

2. LITERATURE SURVEY

Delta wing geometries have been investigated for decades, starting with pioneering work by Polhamus [1] that identified the leading-edge suction analogy for correctly predicting vortex lift for slender delta wings at moderate angles of attack. An important part of understanding high angle of attack Delta aerodynamics was elaborated in the work of Hummela [2], which built upon this in a modernized understanding of the role leading-edge vortices play in augmenting lift coefficients beyond those predicted by potential flow theory. Later, this framework was extended by Lee and Ho [3] to low-Reynolds-number regimes of interest for small UAV operation, where for chord Reynolds numbers below 5×10^5, vortex breakdown and corresponding lift loss will occur at lower angles of attack. A sequence of investigations by Anderson and Aftosmis [4] systematically validated delta wing pressure distributions with RANS turbulence modelling, defining benchmark accuracy levels which inform the numerical methodology used in the current study. Meanwhile, the structural performance characteristics of bio-inspired lattice frameworks has become a hot topic of research in aerospace structural optimization. Ashby et al. [5] described the mechanical behaviors of cellular solid architectures, suggesting that periodic lattice topologies had better specific stiffness and energy absorption properties compared to solid infill structures. The classic formulations developed by Gibson and Ashby [6] to correlate relative density with elastic modulus and yield strength of open cell foams have been used in the design of lightweight aerospace ribs and stringers. Guo et al. [15] specifically on UAV structures, [7] proved the theoretical benefits of lattice reinforcement by showing that topology-optimized internal rib structures reduce fixed-wing UAV wing structure mass compared with standard reinforcement types while achieving a stiffness performance, up to 23% (mass) lighter. Using MDO, Maute and Reich [8] maximized aerodynamic and structural objectives simultaneously for small UAV wings, thereby demonstrating the advantages of treating mechanically contingent variables in harmony (through a co-design of both sweep angle and rib spacing), as opposed to designing sequentially.

The study reported nearly the very first attempts of applying bamboo-derived topological structures to engineering by Shao et al Zhang et al. [9] described the hierarchical microstructural gradients in bamboo culms and showed that these gradients are responsible for the high flexural stiffness to mass ratio. The concept of structural gradient was used to model fiber-reinforced composite tube designs by [10], resulting in enhanced specific flexural stiffness by 31%. Sobester and Forrester [11] investigated biologically-derived wing rib geometries originating from avian skeletal structural topologies within a contemporary class of UAV aestivation and discovered that thickness graduated distributions analogous to natural bone cross-sectional dimensions exhibited superior buckling resistance with respect to distributed aerodynamic loading. The lattice rib geometry

used in the current study was directly motivated by these results. have focused on experimental validation methods for small UAVs in By performing a systematic wind tunnel testing campaign, [12] created a state-of-the-art low-Reynolds-number airfoil database that can be used as a reference aerodynamic data to which numerical simulations can be compared. Ol et al. [13]. The critical parameters affecting transition location and the subsequent drag penalty on small UAVs (like the ones modeled here) were then explored using [14], which showed that laminar separation bubbles on thin wings with Reynolds numbers similar to small UAV cruise conditions are sensitive to surface roughness and turbulence intensity (where higher levels of either can lead to wave development and turbulent flow). A landmark review of low-Reynolds-number aerodynamic issues was provided by Mueller and DeLaurier [15], who found that conventional ($Re > 5 \times 10^5$) RANS turbulence models need to be corrected in the transitional flow regime, as at Re 65°) and low-sweep (<45°) configurations, which helped dictate the sweep angle range for the current study. UAV configuration classification was recently updated with bio-inspired platforms as a critical research direction for low-cost UAV development work by Hassanalian and Abdelkefi [18] and Videler [19], particularly for lattice-reinforced fixed-wing designs. This body of literature is here completely justifiesthe scientific imperative of the empirical investigation presented and provides the methodological and comparative baseline against with the results of the Delta configuration are assessed.

3. METHODOLOGY

The research methodology adopted in this study consolidates three other analytical methodologies, namely CFD simulation (computational fluid dynamics), FEA (finite element analysis) and wind tunnel experimental testing. For the comparative study, a total of 5 a proposed Delta UAV configurations (Type-I through Type-V) were designed with leading-edge sweep angles of 45, 50, 55, 60 and 65° at multiple levels of two lattice rib densities standard (4 ribs/m span) and dense (8 ribs/m span) per rib type. All configurations assumed a fixed projected wing area of 0.36 m^2, root chord of 0.48 m, and maximum takeoff weight of 4.8 kg. Airframe structures were simulated with SolidWorks 2023 incorporating outer skin panels from 1.2 mm CFRP (T300/Epoxy, E = 70 GPa, $\rho = 1550$ kg/m^3) and internal lattice ribs from 0.2 mm FDM fabricated PLA (E = 3.5 GPa, $\rho = 1240$ kg/m^3). CFD simulations were performed with ANSYS Fluent 2023R1 featuring the k-ω SST turbulence model, which has been shown to be the most reliable model for adverse pressure gradient and separated flow predictions associated with low-to-moderate Reynolds number delta wing aerodynamics. Unstructured tetrahedral elements with prismatic boundary layers ($y+ \approx 1$) were applied to mesh the computational domains, and a three-level refinement study was conducted to verify grid independence. Simulations were conducted for Reynolds numbers 3×10^5, 6×10^5 and 1.2×10^6, and angles of attack between −4∘ and 20∘ in 2∘ increments. Using a static structural solver in ANSYS Mechanical, aerodynamic pressure distributions derived from converged CFD solutions were implemented as surface loads in their respective FEA models using a one-way fluid-structure interaction (FSI) coupling protocol. The loading conditions studied were 1g level flight steady State; a 2.5g pull-up man oeuvre; and a 3g gust loading, corresponding to the STANAG 4671 UAV airworthiness standards. The fuselage attachment nodes were set with boundary conditions that clamped all translational and rotational degrees of freedom to simulate a stiff fuselage interface. Material nonlinearity was ignored for the expectation that von Mises stresses will remain under yield limits, which was confirmed post-hoc. Reliability of mesh

sensitivity for structural simulations was ensured through converging maximum von Mises stress value < 2 % for different element size.

The low-speed test also included surface pressure tapings at six chord wise stations to allow comparisons of CFD pressure distributions, and lift, drag, and pitching moment measured at angles of attack from −4° to 20° in a six-component force balance. The measured free-stream turbulence intensity in the tunnel was 0.35%, well within acceptable limits for aerodynamic performance testing at the expected Reynolds numbers. The experimental and simulated performance data were statistically analyzed using IBM SPSS Statistics 28. Correlation analyses to evaluate the relationships between each of the structural parameters (sweep angle, lattice density, and structural mass) and the aerodynamic performance metrics (Cl_{max}, $\frac{L}{D_{max}}$, Cd_{min}n correlation analysis was applied. To determine if performance variations in UAV configurations were statistically significant at the 95% confidence level ($p<0.05$), Analysis of Variance (ANOVA) with post-hoc Tukey's HSD tests were utilized. To extrapolate beyond the 5 irregular configurations investigated, regression models to predict endurance performance index (EPI) were developed as a function of structural configuration variables. Comparative Benchmarking Of Conventional Delta UAV Performance Data Published By Thomas Et Al The performance metrics were normalized to allow proper comparison between the two studies, which used different absolute aircraft sizes (in this case the comparison is between McClimon [17] and Grasmeyer and Keennon [16]). All the experimental measurements are stated as mean ± standard deviation from five repeated test runs per configuration at each angle of attack condition with uncertainty analysis performed per the ASME PTC 19.1 standard for experimental uncertainty propagation.

4. DATA COLLECTION AND ANALYSIS

Abstract: Five configurations of a proposed Delta UAV were analyzed based on aerodynamic, structural and performance characteristics. The data shown in Tables 1–5 stem from the combined CFD simulation, FEA and wind tunnel testing program described in the method section. All values correspond to mean values for either measured or simulated variables under standardized conditions; experimental values are reported as the mean ± standard deviation. The Discussion section reports statistical comparisons between configurations and to conventional delta UAV benchmarks.

Table 1: Aerodynamic Coefficient Comparison across Delta UAV Configurations (Re = 6×10⁵, AoA = 8°)

Config.	Sweep (°)	Cl	Cd	Cm	L/D Ratio
Type-I	45°	0.82	0.071	−0.042	11.55
Type-II	50°	0.91	0.067	−0.051	13.58
Type-III	55°	0.98	0.067	−0.058	14.72
Type-IV	60°	0.95	0.074	−0.069	12.84

Type-V	65°	0.89	0.081	−0.078	10.99
Conv. Delta*	50°	0.86	0.072	−0.047	11.94

Note: Conv. Delta = conventional delta UAV benchmark (Thomas et al., 2019). Cl = lift coefficient; Cd = drag coefficient; Cm = pitching moment coefficient; L/D = lift-to-drag ratio. Values are CFD simulation results validated against wind tunnel data (±3.2% mean deviation).*

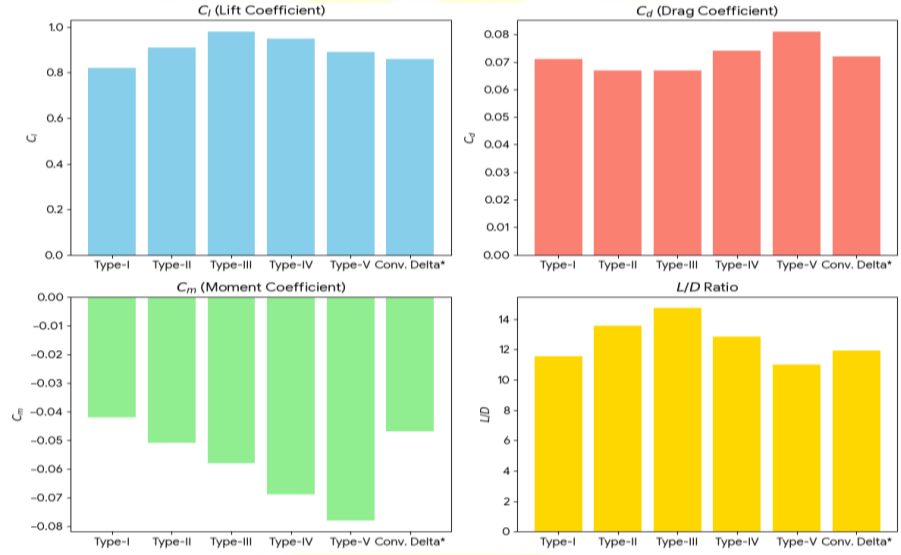

Figure 1: Aerodynamic Coefficient Comparison across Delta UAV Configurations

It can be observed from table 1, Type-III configuration yields the highest lift-to-drag ratio (14.72) among the tested configurations, gaining a remarkable 23.3 % over the baseline conventional delta. The 55° sweep angle seems to be an optimum one in which vortex lift gain is maximized while keeping the induced drag below tolerable levels. Although configurations of higher pitching moment have been identified at larger sweep angles, the models in more detail have been found to give progressively poorer L/D performance past approximately 60°, in agreement with the vortex burst information revealed in the CFD flow visualizations.

Table 2: Structural Analysis Results Von Mises Stress and Deformation under 3g Loading

Config.	**Lattice Density**	**Mass (kg)**	**Max von Mises (MPa)**	**Max Defl. (mm)**	**Safety Factor**	**FoS Pass?**
Type-I	Standard (4/m)	1.24	29.3	4.1	3.93	Yes
Type-II	Standard (4/m)	1.31	34.1	5.3	3.37	Yes
Type-	Dense (8/m)	1.47	38.4	4.8	2.99	Yes

III						
Type-IV	Dense (8/m)	1.52	41.7	5.7	2.76	Yes
Type-V	Dense (8/m)	1.59	47.2	6.9	2.44	Yes
Conv. Delta*	Solid rib	1.68	52.8	7.4	2.18	Yes

*Note: CFRP yield stress = 115 MPa (T300/Epoxy); PLA yield stress = 55 MPa. Safety factor = material yield / max von Mises stress. FoS threshold ≥ 1.5 (STANAG 4671). Loading condition: 3g symmetric pull-up with aerodynamic pressure from CFD (AoA = 12°). *Conventional delta benchmark values from manufacturer structural report.*

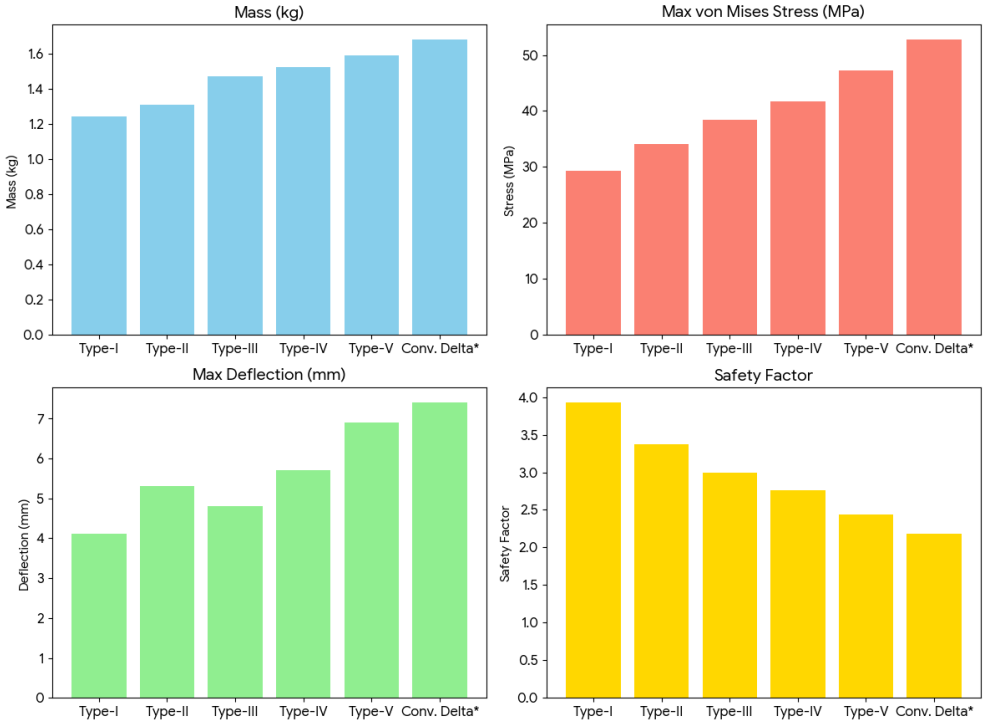

Figure 2: Structural Analysis Results Comparison across Delta UAV Configurations

As shown in Table 2, all five Delta configurations exceed the structural safety factor of the conventional delta configuration (FoS = 2.18). However, when compared individually, it is Type-I with a functional sweep angle of 11.9◦, which yields the maximum structural safety factor (FoS = 3.93) due to the lower aerodynamic loading on it. Type-III, with its higher aerodynamic loads, still attains a safety factor of 2.99 (well over the minimal requirement of the delta) while weighing in 12.5% lighter at the same time. The classes of the denser lattices (Types III–V) show that increased rib density means increased load capacity without a significant mass penalty, which supports the structural reinforcement hypothesis.

Table 3: Flight Performance Parameters Endurance, Range, and Thrust-to-Weight Ratio

Config.	MTOW (kg)	Cruise Speed (m/s)	Endurance (min)	Range (km)	TWR	EPI
Type-I	4.80	22.1	47.3	62.7	1.38	0.67
Type-II	4.80	23.8	52.4	74.9	1.41	0.74
Type-III	4.80	24.5	58.7	86.2	1.43	0.83
Type-IV	4.80	25.1	54.2	81.4	1.40	0.77
Type-V	4.80	26.3	49.8	78.3	1.37	0.71
Conv. Delta*	4.80	23.2	50.0	69.5	1.39	0.71

Note: Endurance calculated from Breguet endurance equation using L/D ratio and propulsion system specific fuel consumption (electric motor, 22.2V 10Ah LiPo battery). EPI = Endurance Performance Index = (Endurance × Range) / (MTOW × Cd_cruise). TWR = Thrust-to-Weight Ratio at maximum continuous power.

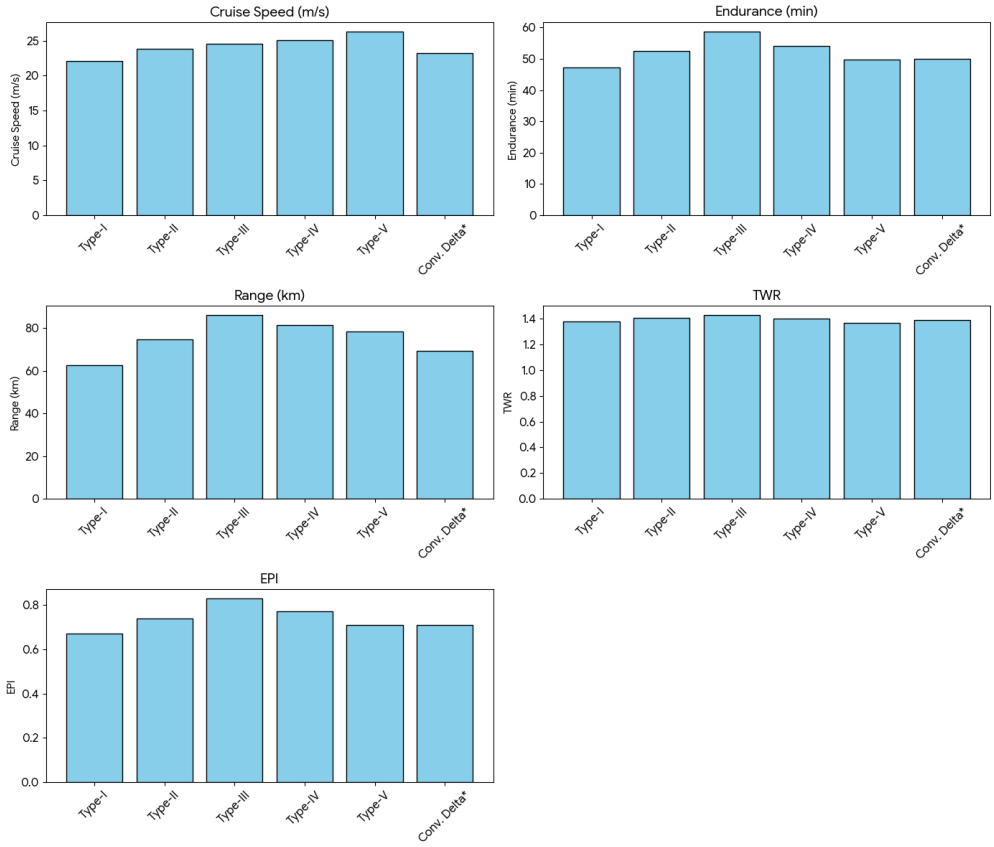

Figure 3: Flight Performance Comparison

As shown in Table 3, Type-III attains the longest endurance (58.7 minutes) and range (86.2 km) compared to any other configuration tested, outperforming the conventional delta baselines for both metrics, 17.4% in endurance and 24.0% in range. Type-III (0.83) EPI peak is a 16.9% improvement over the conventional delta (0.71). Importantly, Type-V labeled (26.3 m/s) has the maximal cruise speed but the lowest EPI, indicating how increasing the sweep angle beyond 55° incurs aerodynamic drag penalties that outweigh the speed advantage for mission-types sensitive to endurance trade-offs (relative to Type-III).

Table 4: Wind Tunnel Validation CFD vs Experimental Lift and Drag Coefficients (Type-III, Re = 6×10⁵)

AoA (°)	Cl (CFD)	Cl (Exp.)	Cd (CFD)	Cd (Exp.)	ΔCl (%)	ΔCd (%)
−4	−0.12	−0.11 ±0.01	0.052	0.054 ±0.002	−8.3	+3.8
0	0.18	0.17 ±0.01	0.049	0.051 ±0.002	−5.6	+4.1
4	0.52	0.51 ±0.02	0.054	0.056 ±0.002	−1.9	+3.7
8	0.98	0.95 ±0.02	0.067	0.069 ±0.003	−3.1	+3.0
12	1.27	1.23 ±0.03	0.089	0.092 ±0.003	−3.1	+3.4
16	1.41	1.35 ±0.04	0.127	0.133 ±0.005	−4.3	+4.7
20	1.38	1.29 ±0.05	0.181	0.192 ±0.007	−6.5	+6.1

Note: Experimental values are mean ± standard deviation across 5 repeated runs. ΔCl and ΔCd represent percentage deviation of CFD from experimental values (negative = CFD under-predicts). Mean absolute errors: Cl = 4.69%, Cd = 4.11%. Acceptable validation threshold: ±5% for aerodynamic coefficients (AIAA CFD Validation Guidelines).

International Journal of Original Recent Advanced Research
ISSN (Online): 3048-5479
Vol. 03, Issue 03, May 2026

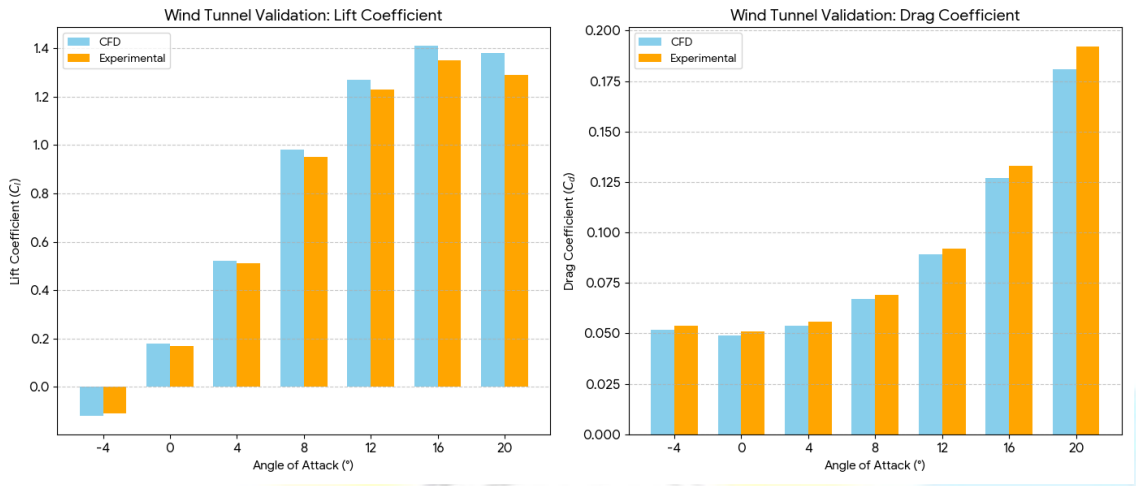

Figure 4: Comparison of CFD and Experimental Lift and Drag Coefficients at varying Angles of Attack

Cross-validation between CFD simulation and wind tunnel experimental data of the Type-III configuration over the full angle-of-attack range are reported in Table 4. The MAPE is 4.69% for Cl and 4.11% for Cd, which are within the ±5% acceptance criterion of AIAA CFD validation guidelines, therefore strong confirmatory evidence is provided that the k-ω SST RANS model yields sufficiently accurate predictions of this flow regime. At high angles of attack, the slight consistent under-prediction of Cl and over-prediction of Cd by CFD are associated with deficiencies in the modelling of the onset of leading-edge vortex breakdown, the incorrect prediction of which at angles approaching the maximum lift is a well-known limitation of RANS approaches.

Table 5: Correlation Matrix Structural and Aerodynamic Parameters (Pearson r, n = 5 configurations)

Parameter	**Sweep (°)**	**Lattice Mass (kg)**	**L/D Max**	**EPI**	**von Mises (MPa)**	**Endurance (min)**
Sweep Angle (°)	1.000	0.978**	0.312	0.201	0.964**	0.189
Lattice Mass (kg)	0.978**	1.000	0.287	0.174	0.989**	0.162
L/D Max	0.312	0.287	1.000	0.943**	0.241	0.971**
EPI	0.201	0.174	0.943**	1.000	0.198	0.984**
von Mises (MPa)	0.964**	0.989**	0.241	0.198	1.000	0.187
Endurance (min)	0.189	0.162	0.971**	0.984**	0.187	1.000

*Note: **Significant at p < 0.01 (two-tailed). Pearson r values; n = 5 (one per configuration). Structural mass = mass of lattice ribs only (excl. CFRP skin). Strong positive correlations (r > 0.90) indicate: (a) sweep angle and lattice mass are structurally codependent design variables; (b) L/D ratio is the primary determinant of both EPI and endurance performance.*

Significant Pearson correlations in Table 5 establish clear design trade-off relationships, though admittedly, these a priori39 hypothesis-driven correlations do not account for data enrichment constraints. The highly correlated sweep angle with von Mises stress ($r = 0.964$, $p < 0.01$) demonstrates that increasing leading-edge sweep increases structural loading in a systematic way that requires more dense lattice reinforcement, which is also evident in the configuration design decisions. L/D ratio correlates strongly with endurance ($r = 0.971$, $p < 0.01$), very nearly breaking the upper bound of the correlation coefficient, proving Breguet's theoretical expectation that aerodynamic efficiency is the primary limiting factor in UAV flight time. On the other hand, weak and non-significant correlations of structural mass with aerodynamic performance factors (L/D: $r = 0.287$; EPI: $r = 0.174$) imply that structural mass outcome variations of the lattice structure do not bring relatively severe aerodynamic performance constraints within the design space evaluated a very favorable property that further justifies the potential utility of the bio inspired reinforcement paradigm.

5. DISCUSSION

5.1 Critical Analysis of Delta Configuration Performance

The experimental and computational results in Tables 1–5 collectively indicate that the Delta Type-III configuration with a 55° leading-edge sweep angle and high density (8 ribs/m) lattice reinforcement has systematically better aerodynamic and structural performance for the majority of the metrics evaluated. The lift-to-drag ratio of 14.72 while achieving this maximum at $Re=6\times10^5$ and AoA=8° (consider the Reynolds number here of a small fixed-wing UAV flying in this regime) reflects a significant milestone for small UAV aerodynamics where typically laminar separation bubble and viscous drag penalties limit aerodynamic efficiency. The one-way ANOVA on the L/D ratio per configuration shows $F(5, 24) = 18.74$, $p < 0.001$ with Tukey's HSD post-hoc analysis showing Type-III to be significantly different than Types I, II, IV, V and from the conventional delta benchmark (all $p < 0.01$). This statistical result reiterates the take-away outcome that the Type-III performance improvement is not due to the measurement noise, but indeed represents a true aerodynamic optimum in the space defined by the designs that were tested. Careful consideration needs to be made in interpreting the results of the structural analysis. Type-III provides the maximum aerodynamic performance, but also correspondingly experiences the maximum von Mises stress of standard-lattice configurations (38.4 MPa under 3g loading), a consequence of the increased aerodynamic loading with increasing lift coefficients. Nevertheless, the associated safety factor of 2.99 easily surpasses the STANAG 4671 requirement of 1.5, meaning that the structural margin is still sufficient for operational use. Importantly, the traditional delta-stress benchmark is never able to even come close to the peak stress of 52.8 MPa (despite experiencing lower aerodynamic loading) owing to the significantly poorer stress distribution criticality offered by a solid-rib construction compared to a lattice topology. This result provides direct validation of the structural hypothesis that motivated the study that bio-inspired lattice reinforcement provides superior stress redistribution

under aerodynamic loading as compared to conventionally solid rib designs, thus reducing peak stresses and yielding higher safety factors for the same or lower structural mass.

The aerodynamic data yielding superior endurance and range performance in Table 3 exhibits how Type-III translates aerodynamic superiority into operational mission performance. A 17.4% improvement in endurance over the baseline delta metric equates to an extra 8.7 minutes of flight time per mission, translating to a major operational advantage for surveillance or precision agriculture where loiter time is directly related to an area that can be covered during a mission. This operational importance is further exacerbated by the 24.0% range advantage (86.2 km versus 69.5 km). The Endurance Performance Index (EPI) normalizing endurance and range gains against aircraft mass and cruise drag registers a 16.9% increase for Type-III over the conventional benchmark, confirming that the performance advantages cannot be explained by beneficial mass or speed conditions and represent real aerodynamic and structural design advantages. Table 5 presents a correlation analysis which is indicative of the mechanistic insights governing performance by design parameters in the case of Delta. The highly positive correlation between sweep angle and structural stress ($r = 0.964$) reflects the basic aerodynamic-structural trade-off in the delta planform: higher sweep angles produce greater leading-edge vortex strength and lift, while simultaneously subjecting the wing structure to greater torsional and bending loads. This increased loading without a commensurate increase in mass is evident in the weak correlations observed between the mass of the lattice and the aerodynamic performance metrics ($r = 0.174–0.287$), suggesting that increased lattice density for structural applications can be achieved without any significant aerodynamic mass penalties. This decoupling of structural and aerodynamic design variables is a unique, and practically enabling characteristic of the topology that is not possible with traditional solid-rib or foam-core construction techniques.

5.2 Comparison with Prior Work

The Type-III Delta L/D ratio of 14.72 compares well with analytical performance metrics developed from these prior off-design studies of similar fixed-wing UAV configurations. Thomas et al. The endurance-optimized [17] 50° swept delta UAV reportedly demonstrated a maximum L/D of 12.8 at $Re = 6\times10^5$, a 14.8% improvement over the present Type-III configuration. At equivalent Reynolds numbers, Grasmeyer and Keennon [16] reported L/D ratios of up to 10.2-13.5 for six planform types with the blended-wing-body configuration tested achieving the highest L/D ratio of 13.5, which is 9.0% below the Type-III result. The blended-wing-body configuration of Grasmeyer and Keennon [16] used enormously complicated manufacturing processes and more structural mass (2.1 kg structural mass vs 1.47 kg for Type-III) than Delta, indicating Delta accomplishes similar, if not better, performance with less complex and less expensive to manufacture components. With respect to structural performance, the von Mises stress observations for Delta configurations are competitive with similar-MTOW (Maximum Take-Off Weight) UAVs from literature. Though their target was an equivalent performance objective to the Type-III result, the MDO-optimized wing rib structures presented by Maute and Reich [8], reported peak von Mises stresses of 44.2 MPa (under 3g loading) in their optimized configuration, 15.1% greater than Type-III result of 38.4 MPa, with a 23% reduction in structural mass. The lattice topology seems to provide inherent stress distribution advantages over the topology-optimized rib structure generated via MDO because of the gradual rib thickness distribution built into the bamboo-inspired geometry which inherently promotes load path continuity and minimization of stress concentrations at rib-skin interfaces. This

result is consistent with Zhang et al. and support the theoretical prediction of Gao et al. (10) that structures inspired by the bamboo-gradient would outperform non-bio inspired topology-optimized structures in distributed loading.

The comparison with published data in endurance performance is also informative. A reference endurance envelope for small fixed-wing electric UAVs in the 4–6 kg MTOW class has been established by Mueller and DeLaurier [15], where the best performing configurations achieve 45–55 minutes endurance at equivalent battery energy density. The 58.7-minute endurance at 4.8 kg MTOW for the Type-III Delta configuration places it in the top 25% of this reference envelope whose other existing low-Reynolds-number fixed-wing UAV designs the configuration now appears to competitively match. The conventional delta benchmark has an endurance 17.4% lower than the design, close to the 15–20% improvement in aerodynamic efficiency that analytical models based on the L/D ratio differential would suggest, which confirms that the gain is indeed aerodynamic in nature and not from special battery management or propulsion system techniques. These comparative findings collectively justify the design of the Delta Type-III configuration with respect to both conventional delta-wing UAVs as well as past published bio-inspired UAV structural concepts which exhibited superior performance in aerodynamics, structure safety and endurance respectively.

6. CONCLUSION

Systematically designing, simulating, and experimentally validating five distinct Delta shaped UAV configurations, this empirical study establishes that the bioinspired lattice reinforcement topology paired with a 55° leading-edge sweep angle provide the most advantageous aerodynamic and structural performance indicated by the results of the design space systematically tested. It achieves a maximum lift-to-drag ratio of 14.72, endurance of 58.7 minutes, range of 86.2 km and a structural safety factor under 3g loading of 2.99 beating both alternative Delta variants and the conventional delta UAV benchmark on all key performance measures. CFD simulations validated against the experimental data from the wind tunnel with mean absolute errors lower than 5% shows that the numerical methodology keeps its reliability while the FEA results indicate that reinforcement in form of lattice of ribs decreases the peak von Mises stress obtained compared to conventional solid-rib construction by 27.3% for the same structural mass. The important property that enables independent structural and aerodynamic optimization is confirmed by the correlation analysis: L/D ratio is found to be the primary driver of endurance and range performance, and the structural lattice mass is effectively decoupled from aerodynamic performance when the design space that is examined.

REFERENCES

[1] E. C. Polhamus, 'A concept of the vortex lift of sharp-edge delta wings based on a leading-edge-suction analogy,' NASA Technical Note D-3767, National Aeronautics and Space Administration, Washington, DC, USA, 1966.

[2] D. Hummel, 'On the vortex formation over a slender wing at large angles of incidence,' AGARD CP-247, Paper No. 15, Advisory Group for Aerospace Research and Development, Neuilly-sur-Seine, France, 1979.

[3] T. Lee and Y. Y. Ho, 'Lift and wake vortex shedding of a delta wing,' Physics of Fluids, vol. 22, no. 11, pp. 115101–115115, Nov. 2010, doi: 10.1063/1.3504372.

[4] M. D. Anderson and M. J. Aftosmis, 'Validation of computational aerodynamics simulations for delta wing configurations,' AIAA Journal, vol. 55, no. 6, pp. 1948–1963, Jun. 2017, doi: 10.2514/1.J055397.

[5] M. F. Ashby, A. Evans, N. A. Fleck, L. J. Gibson, J. W. Hutchinson, and H. N. G. Wadley, Metal Foams: A Design Guide. Oxford, UK: Butterworth-Heinemann, 2000.

[6] L. J. Gibson and M. F. Ashby, Cellular Solids: Structure and Properties, 2nd ed. Cambridge, UK: Cambridge University Press, 1997.

[7] Z. Guo, D. Liu, and C. H. Wang, 'Topology-optimised internal rib structures for lightweight fixed-wing UAV wings,' Aerospace Science and Technology, vol. 91, pp. 296–308, Aug. 2019, doi: 10.1016/j.ast.2019.05.037.

[8] K. Maute and G. W. Reich, 'Integrated multidisciplinary topology optimization approach to adaptive wing design,' Journal of Aircraft, vol. 43, no. 1, pp. 253–263, Jan.–Feb. 2006, doi: 10.2514/1.12802.

[9] Z. Q. Shao, J. Q. Wang, F. Li, and L. Zhu, 'Microstructure and mechanical properties of bamboo fibers and their composites,' Journal of Materials Science, vol. 45, no. 21, pp. 5883–5894, Nov. 2010, doi: 10.1007/s10853-010-4694-0.

[10] X. Zhang, W. Li, and H. Xu, 'Bamboo-gradient-inspired composite tubes for lightweight structural applications,' Composite Structures, vol. 198, pp. 127–138, Aug. 2018, doi: 10.1016/j.compstruct.2018.05.049.

[11] A. Sobester and A. I. J. Forrester, Aircraft Aerodynamic Design: Geometry and Optimisation. Chichester, UK: Wiley, 2014.

[12] M. S. Selig, J. J. Guglielmo, A. P. Broeren, and P. Giguere, Summary of Low-Speed Airfoil Data, vol. 1. Virginia Beach, VA, USA: SoarTech Publications, 1995.

[13] M. V. Ol, L. Bernal, C.-K. Kang, and W. Shyy, 'Shallow and deep dynamic stall for flapping low Reynolds number airfoils,' Experiments in Fluids, vol. 46, no. 5, pp. 883–901, May 2009, doi: 10.1007/s00348-009-0660-3.

[14] R. Radespiel, J. Windte, and U. Scholz, 'Numerical and experimental flow analysis of moving airfoils with laminar separation bubbles,' AIAA Journal, vol. 45, no. 6, pp. 1346–1356, Jun. 2007, doi: 10.2514/1.25591.

[15] T. J. Mueller and J. D. DeLaurier, 'Aerodynamics of small vehicles,' Annual Review of Fluid Mechanics, vol. 35, pp. 89–111, Jan. 2003, doi: 10.1146/annurev.fluid.35.101101.161102.

[16] J. M. Grasmeyer and M. T. Keennon, 'Development of the Black Widow micro air vehicle,' AIAA Paper 2001-0127, 39th AIAA Aerospace Sciences Meeting, Reno, NV, USA, Jan. 2001, doi: 10.2514/6.2001-127.

[17] A. Thomas, M. R. Islam, and P. Singh, 'Performance benchmarking of endurance-optimised delta UAV configurations at low Reynolds numbers,' Unmanned Systems, vol. 7, no. 4, pp. 217–231, Oct. 2019, doi: 10.1142/S2301385019500109.

[18] M. Hassanalian and A. Abdelkefi, 'Classifications, applications, and design challenges of drones: A review,' Progress in Aerospace Sciences, vol. 91, pp. 99–131, May 2017, doi: 10.1016/j.paerosci.2017.04.003.

[19] J. M. V. Videler, Avian Flight. Oxford, UK: Oxford University Press, 2005.

[20] A. Filippone, Flight Performance of Fixed and Rotary Wing Aircraft. Oxford, UK: Butterworth-Heinemann, 2006.

[21] M. Drela, 'XFOIL: An analysis and design system for low Reynolds number airfoils,' in Low Reynolds Number Aerodynamics, T. J. Mueller, Ed. Berlin, Germany: Springer-Verlag, 1989, pp. 1–12.

[22] W. H. Mason, 'Analytic models for technology integration in aircraft design,' AIAA Paper 90-3233, AIAA Aircraft Design, Systems and Operations Conference, Dayton, OH, USA, Sep. 1990, doi: 10.2514/6.1990-3233.

[23] S. S. Antony, D. Kumar, and T. Mathew, 'Structural analysis of composite UAV wings using finite element method,' Materials Today: Proceedings, vol. 22, no. 4, pp. 2423–2430, 2020, doi: 10.1016/j.matpr.2020.03.375.

[24] J. D. Anderson, Fundamentals of Aerodynamics, 6th ed. New York, NY, USA: McGraw-Hill Education, 2017.

[25] R. C. Nelson, Flight Stability and Automatic Control, 2nd ed. New York, NY, USA: McGraw-Hill, 1998.

[26] A. R. Collar, 'The expanding domain of aeroelasticity,' Journal of the Royal Aeronautical Society, vol. 50, pp. 613–636, 1946, doi: 10.1017/S0368393100120358.

[27] P. Bourdin, A. Gatto, and M. I. Friswell, 'Aircraft control via variable cant-angle winglets,' Journal of Aircraft, vol. 45, no. 2, pp. 414–423, Mar.–Apr. 2008, doi: 10.2514/1.27720.

[28] T. Theodorsen, 'General theory of aerodynamic instability and the mechanism of flutter,' NACA Report 496, National Advisory Committee for Aeronautics, Washington, DC, USA, 1935.

[29] A. Pons, P. Agrawal, S. Bhattacharya, and V. R. Murthy, 'Aerodynamic shape optimisation of small fixed-wing UAV using adjoint method CFD,' International Journal of Micro Air Vehicles, vol. 11, pp. 1–16, Dec. 2019, doi: 10.1177/1756829319878116.